

Pulses in the Zero-Spacing Limit of the GOY Model

K.H. Andersen ^a, T. Bohr ^b, M.H. Jensen ^c, J.L. Nielsen ^c and
P. Olesen ^c

^a*Department of Hydrodynamics and Water Resources (ISVA), the Danish Technical University, building 115, DK-2800 Lyngby, Denmark, tlf.: +45 45251420, fax: +45 45932860, e-mail: ken@isva.dtu.dk, www.isva.dtu.dk/~ken.*

^b*Department of Physics, the Danish Technical University, building 309, DK-2800 Lyngby, Denmark*

^c*The Niels Bohr Institute, Blegdamsvej 17, DK-2100 Copenhagen Ø, Denmark*

Abstract

We study the propagation of localised disturbances in a turbulent, but momentarily quiescent and unforced shell model (an approximation of the Navier-Stokes equations on a set of exponentially spaced momentum shells). These disturbances represent bursts of turbulence travelling down the inertial range, which is thought to be responsible for the intermittency observed in turbulence. Starting from the GOY shell model, we go to the limit where the distance between succeeding shells approaches zero (“the zero spacing limit”) and helicity conservation is retained. We obtain a discrete field theory which is numerically shown to have pulse solutions travelling with constant speed and with unchanged form. We give numerical evidence that the model might even be exactly integrable, although the continuum limit seems to be singular and the pulses show an unusual super exponential decay to zero as $\exp(-\text{const } \sigma^n)$ when $n \rightarrow \infty$, where σ is the *golden mean*. For finite momentum shell spacing, we argue that the pulses should accelerate, moving to infinity in a finite time. Finally we show that the maximal Lyapunov exponent of the GOY model approaches zero in this limit.

Key words: Pacs: 47.27.Gs, 05.45.Yv.

Keywords: Turbulence, shell model, GOY model, continuum limit.

Shell models of turbulence have increasingly been used as a laboratory for testing hypotheses about the statistical nature of Navier-Stokes turbulence. Even though they are derived by heuristic arguments they are surprisingly adept at reproducing the statistical properties of high Reynolds number turbulence. The reasons behind the apparent success of the shell models still

remains unclear. In the present paper an attempt will be made to examine the detailed behaviour of one particular shell model – the so-called GOY model by Gledzer-Ohkitani-Yamada [1–10] in the limit where the ration between the wave number of successive shells approach unity – which we shall refer to as the zero-spacing limit.

One of the most important problems in turbulence is to understand *intermittency* – the very lumpy and irregular intensity of turbulent motion. Even in strongly turbulent states each region experiences periods of almost complete quiescence interrupted by rapid burst events, and this is believed to be the origin of the corrections to Kolmogorov scaling seen experimentally, and predicted rather accurately by the shell models [3]. Single burst motion superimposed on the Kolmogorov spectrum (which emerges as a fixed point of the shell model) have been studied in shell models by a number of authors [11–14]. In this paper we also consider single burst motion but, in contrast to the previous work, we do not superimpose a Kolmogorov background. It was shown recently, that prior to a burst in the GOY shell model, the velocity field tends toward the “trivial” quiescent fixed point [15]. In this paper we thus study localised disturbances propagating through the quiescent, unforced system. One should keep in mind in the following, that the shell models are defined in k -space and that the pulses we describe are likewise in k -space. Thus a pulse travelling to smaller k should correspond roughly to a spatial region of growing size, but we shall not go into the detailed conversion of our results to real space, since this is not even a completely well defined process in the context of (1-d) shell models.

The paper is structured as follows: First a short introduction to the GOY model is given in Section 1. It was conjectured by Parisi in a yet unpublished paper [12] that the correlation functions of the GOY model (also called the structure functions) might be calculated from the existence of soliton-like solutions on top of the Kolmogorov fixed point $u(k) \propto k^{-1/3}$. For the study of the pulses he proposed a continuum limit of the GOY model (the “Parisi equation”). Around the quiescent fixed point this equation does not form pulses, but rather forms shocks. The Parisi equation around the quiescent fixed point is studied in [16] and the results are briefly reviewed in section 2. Pulses in the quiescent state are, however, seen in the zero-spacing limit of the GOY model. The equation governing the zero-spacing limit is derived in section 3 and the qualitative behaviour of our model is illustrated through numerical simulations. In section 4 a continuum version of the zero-spacing limit is proposed, and a solution for a pulse is derived. The asymptotic behaviour of a pulse is is treated in the case where the background field is zero (section 5) and non-zero (section 6). In section 7 the acceleration of a pulse which is seen away from the zero-spacing limit is examined. Finally the Lyapunov exponent of the GOY model is calculated as a function of the shell spacing, and it is shown that the model is not chaotic in the limit of the shell spacing going

towards zero (Section 8)

1 The GOY model

Shell models are formed by a truncation approximation (in k -space) of the Navier-Stokes equations [10]. The most well-studied model is the “GOY” model of Gledzer-Ohkitani-Yamada.

This model yields corrections to the Kolmogorov theory [3] in good agreement with experiments [17,18]. For the “GOY” shell model, wave-number space is divided into N separated shells each characterised by a wave-number $k_n = r^n k_0$ with $n = 1, \dots, N$. Each shell is assigned a complex amplitude u_n describing the typical velocity difference over a scale $\ell_n = 1/k_n$. By assuming interactions only among nearest and next nearest neighbour shells and phase space volume conservation one arrives at the following evolution equations [2]

$$\left(\frac{d}{dt} + \nu k_n^2\right) u_n = i k_n \left(a_n u_{n+1}^* u_{n+2}^* + \frac{b_n}{r} u_{n-1}^* u_{n+1}^* + \frac{c_n}{r^2} u_{n-1}^* u_{n-2}^* \right) + f, \quad (1)$$

with boundary conditions $b_1 = b_N = c_1 = c_2 = a_{N-1} = a_N = 0$. f is an external, constant forcing, and ν is the viscosity.

An important property of the GOY model is that it is possible to incorporate the conservation laws of turbulence as found in the Navier-Stokes equations. The first conservation law that needs to be satisfied is the conservation of energy. The energy in the GOY model is given by

$$E = \sum_n |u_n|^2 \quad (2)$$

which should be conserved in the limits of no forcing and vanishing viscosity. This leads to the following relation between the coefficients

$$a_n + b_{n+1} + c_{n+2} = 0 \quad (3)$$

The constraint still leaves a free parameter δ so that one can set $a_n = 1$, $b_{n+1} = -\delta$, $c_{n+2} = -(1 - \delta)$ [9] (the value of a_n is fixed by the time scale). Kadanoff *et al.* [6] observed that also a “helicity” invariant exists on the form

$$H = \sum_n (-1)^n k_n |u_n|^2 \quad (4)$$

Conservation of this quantity leads to an additional constraint on the parameter b_n

$$b_n = \frac{1}{r} - 1 \quad \text{or} \quad \delta = 1 - \frac{1}{r}. \quad (5)$$

In the most studied case where $r = 2$ one obtains the canonical values $b_n = c_n = \frac{1}{2}$. In this paper we are going to focus on the limiting case $r \rightarrow 1$ and according to Eq. (5) $b_n \rightarrow 0$ in order to satisfy helicity conservation. The set (1) of N coupled ordinary differential equations can be numerically integrated by standard techniques.

2 Some results on the Parisi continuum limit

In a previous paper [16] we studied a number of features of the Parisi [12] continuum model. In particular, a “burst” event (the evolution of an initial condition having support only in a finite interval of k -space) was studied. The initial burst splits up into a right and a left moving part and on the front of each part a shock is formed. It was shown that the continuum equation without forcing or dissipation can be explicitly written in characteristic form and that the right and left moving parts can be solved exactly. When this is supplemented by the appropriate shock condition it is possible to find the asymptotic form of the burst.

In this section we shall give a brief review of some of the main features previously obtained. The continuum Parisi equation is obtained from the GOY model by letting the shell spacing approach zero, and expanding to the first order. By writing the distance between the shells as $r = 1 + \epsilon$ with $\epsilon \ll 1$, we have $k_n \approx \exp(n\epsilon)$, so with $n \sim \text{const.}/\epsilon$ a continuous range of values is obtained for the variable k .

To proceed we use a Taylor expansion of the type

$$\begin{aligned} u_{n+1}(t) &= u(k_{n+1}, t) = u(\ln k_{n+1}, t) \approx u(n \ln(1 + \epsilon), t) + \ln(1 + \epsilon) \frac{\partial u_n}{\partial \ln k} \\ &\approx u(k, t) + \epsilon k \frac{\partial u(k, t)}{\partial k} \\ &= u(k, t) + \epsilon k \frac{\partial u(k, t)}{\partial k}, \quad \text{with } u(k, t) \equiv u(k_n, t) = u_n(t), \end{aligned} \quad (6)$$

and similarly for u_{n+2} , u_{n-1} , and u_{n-2} . To first order one obtains [12]:

$$u_t^* + \nu k^2 u^* = -ik(2 - \delta) (u^2 + 3kuu_k), \quad (7)$$

where $u_k \equiv \partial u / \partial k$ etc.. By rescaling time with $2-\delta$ we get the Parisi equation:

$$u_t^* + 3ikuu_k = -iku^2, \quad (8)$$

for the case of no forcing or viscosity. Here subscripts denote differentiation. Splitting into real and imaginary parts, $u = a + ib$, we get

$$a_t - 3kab_k - 3kab_k = 2kab \quad (9)$$

and

$$b_t - 3kaa_k + 3kbb_k = k(a^2 - b^2). \quad (10)$$

In numerical simulations we observed that a short while after the initialisation, shocks are formed in both directions. As was seen from the equations, the real part is only able to move to the left, while the imaginary part moves both ways. Setting $a = 0$ in the original equations, we get just a single real equation for the inertial range:

$$b_t + 3k^2bb_k = -kb^2 \quad (11)$$

For the left-moving part of the pulse, the real and the imaginary parts are seen to become proportional. Inserting $b = Ca$ into the Parisi equation gives us two possibilities: $a = 0$ (which we already treated) and $a = \pm\sqrt{3}b$. For $a = \sqrt{3}b$ the equation for the imaginary part becomes:

$$b_t - 6k^2bb_k = 2kb^2. \quad (12)$$

It is possible to explain the observed splitting of the pulse by writing (8) in characteristic form. We shall not give the details, since they can be found in the previous paper [16]. The starting point is to rewrite (8) in a form resembling the the Burgers equation

$$v_t^* - ivv_x = 0, \quad (13)$$

where $u = k^{-1/3}v$ and $k = (2x)^{-3/2}$. Of course, there are three important differences to the Burgers equation: Here we have an equation in k -space, v is complex and the conserved quantity is the energy $E = \int (2x)^{5/2}v^2$. Writing $v = re^{i\theta/3}$ the Riemann invariants J_{\pm} can be found, and the solution can be expressed in terms of these

$$r = \left(\frac{J_+^3 + J_-^3}{2} \right)^{1/3}, \quad (14)$$

and

$$\sin \theta = \frac{J_+^3 - J_-^3}{J_+^3 + J_-^3}. \quad (15)$$

The formulation in terms of characteristics can now be used to understand the splitting of the pulse found in Section 3.1. The Riemann invariants J_{\pm} have the property that they are constant along the curve:

$$\frac{dx}{dt} = \pm r(x, t). \quad (16)$$

The important point is that, since r is nonnegative, one family of characteristics (J_+) can never move to the left while the other one (J_-) can never move to the right. If the initial condition has support in a limited region of x , say $[x_-, x_+]$ the same is true of J_{\pm} . They both vanish (in the initial condition) outside of this interval. For times $t > 0$ we compute the field values by finding where, on the x -axis (i.e., $t = 0$), the characteristics going through the point (x, t) emanate. Now, if $x > x_+$, the J_- -characteristic going through this point must emanate from some $x_0 > x_+$ and thus $J_-(x, t) = J_-(x_0, 0) = 0$. This means that either $r = 0$ (which makes the entire field vanish) or $\sin \theta = 1$ which means that θ has the constant value $\pi/2$, which implies that $a = 0$, in agreement with the numerical simulations.

The splitting of the pulse into a right-moving part with $a = 0$ and a left-moving part with $a = \sqrt{3}b$ makes it possible to give a complete solution for a single burst event. For the details, we refer to [16]. Each pulse develops a shock which can be followed by imposing conservation of energy across the shock.

The asymptotical solutions for the two pulses are:

$$u_{right} = (2t)^{-2/3} k^{-1/3} \quad (17)$$

$$u_{left} = (tk)^{-1} \quad \text{down to } k \sim C/t \quad (18)$$

both decaying in time. Thus a burst created on top of the zero solution not only travels down the inertial range until it is dissipated by viscosity (here, by the continuum), it also travels upwards, to the smallest k . The burst does not remain localised in k -space, but is distributed over the k -range, and then decays. It is interesting to note that the initial disturbance creates both a forward and an inverse cascade.

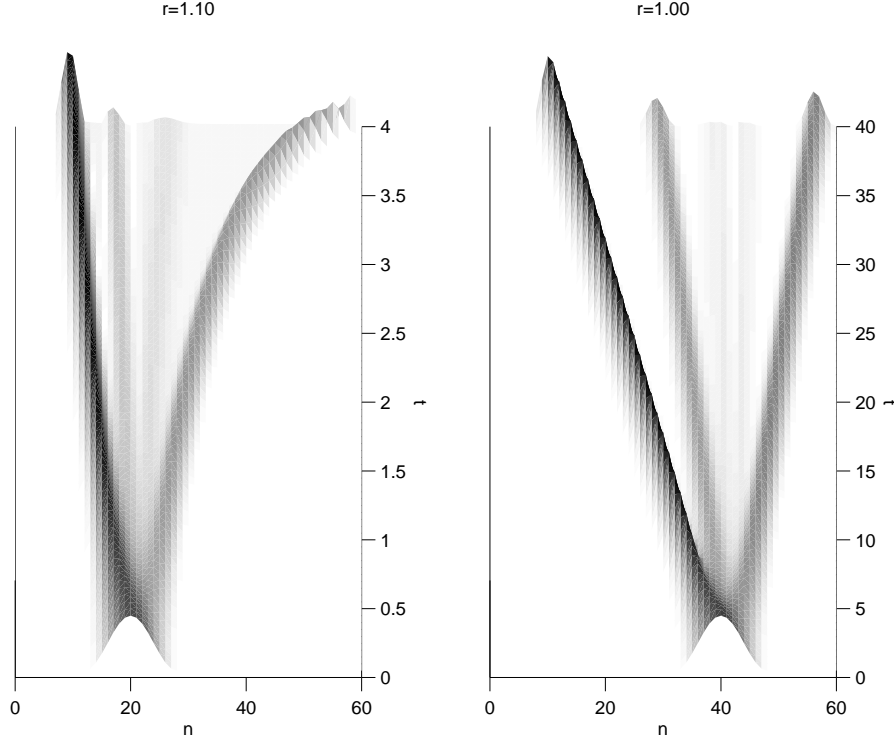


Fig. 1. The development of a initial small bump in the GOY model with $r = 1.1$ and $r = 1.0$. Shown is $|u_n|$.

3 The zero-spacing limit

When we study the GOY model for $r \geq 1$ we observe important deviations from the behaviour of the Parisi equation described in the previous section. We focus on the motion on a single pulse in the case where both the forcing and the viscosity is zero, i.e., $\nu = f = 0$ and the two cases $r = 1.0$ and $r = 1.1$ (Fig. 1). the initial condition is a localised bump:

$$u_n = u_0(1 + i) \{ \cos[(n - n_0)\kappa_0] + 1 \} \quad \text{for } x \in [n_0\kappa_0 - \pi, n_0\kappa_0 + \pi], \quad (19)$$

where n_0 is the center of the bump, $2\pi\kappa_0$ is the length of the bump and $\frac{1}{2}u_0$ is the height of the bump.

The initial bump splits up into a left and a right moving part with the same phases as in the Parisi equation. However, a shock is not formed, rather the initial bump splits into a number of individual pulses. In the case $r = 1.10$, the pulse to the right accelerates whereas the pulse moving to the left decelerates, similar to the shocks in the Parisi equation. In the case $r = 1$, this does not happen and both *the right- and left-moving pulses propagate with a constant velocity*. In both cases, however, the shapes *stays invariant as time progresses*, completely similar to the behaviour of a soliton in an integrable system, like

the KdV equation.

To be able to observe the pulses in more detail, we perform the limit $r \rightarrow 1$ in a different way as is done when the Parisi equation is derived. We shall show that this leads to an interesting model containing pulses moving with constant velocity and which might even be a new example of a completely integrable discrete field theory.

The starting point is the GOY model

$$\left(\frac{du_n}{dt} + \nu k_n^2 u_n\right)^* = -ik_n(u_{n+1}u_{n+2} - \frac{\delta}{r}u_{n-1}u_{n+1} - \frac{1-\delta}{r^2}u_{n-1}u_{n-2}) \quad (20)$$

where $k_n = k_0 r^n$. We now introduce the variable $w_n = k_{n-1}u_n$, and in terms of this variable we get

$$\left(\frac{dw_n}{dt} + \nu k_n^2 w_n\right)^* = -i(r^{-2}w_{n+1}w_{n+2} - \delta w_{n-1}w_{n+1} - (1-\delta)r^2 w_{n-1}w_{n-2}) \quad (21)$$

Using this substitution we get rid of the explicit dependence on k_n on the right hand side of Eq. (21).

Now we take the limit $r \rightarrow 1$ and at the same time we invoke *helicity conservation*, which means that we must choose $\delta = 1 - 1/r \rightarrow 0$. Finally, we are interested in very large Reynolds numbers, so we let $\nu \rightarrow 0$ and then we arrive at the model

$$\frac{dw_n^*}{dt} = -i(w_{n+1}w_{n+2} - w_{n-1}w_{n-2}) \quad (22)$$

The middle term in the GOY model has disappeared and we are left with the two terms directly responsible for the propagation of the pulses to the left and the right.

This model has turned out to have very interesting properties. An initial bump on zero background ($w = 0$) splits into a series of left and right moving pulses with constant velocity as already shown in Fig. 1. Similar to the case for the Parisi equation (8) the phases of the pulses only have certain fixed values. Let

$$w_n = R_n e^{i\phi} \quad (23)$$

then

$$\frac{dR_n}{dt} = (R_{n+1}R_{n+2} - R_{n-1}R_{n-2})e^{i(3\phi-\pi/2)} \quad (24)$$

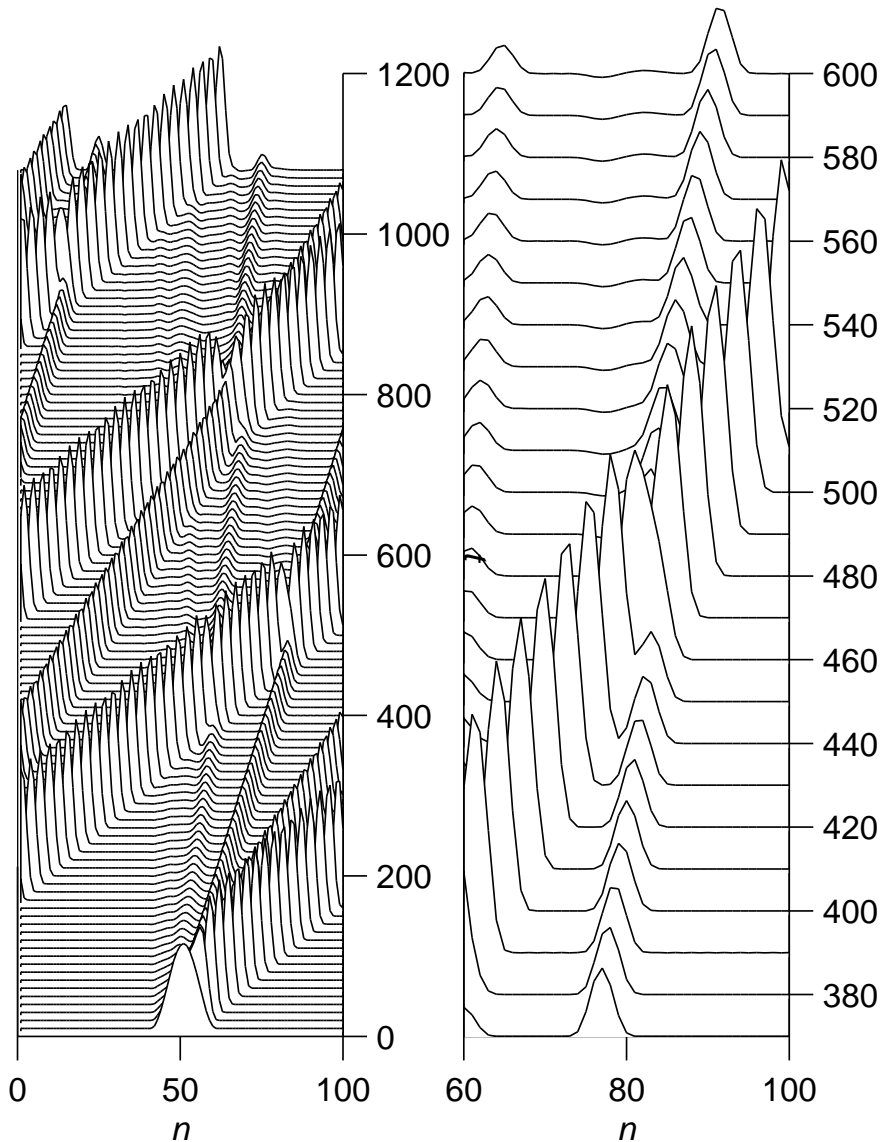


Fig. 2. Time-space plots of the imaginary part of the transformed GOY model Eq. (26), with a cosine-bump as initial condition (19). The boundary conditions are made periodic, to make it possible to see the interaction of the pulses. The right picture is a zoom on an interaction between two pulses, where the time-delay in the collision process is clearly visible

and to have a solution with constant phase, the exponential factor has to be real. This means that $\sin(3\phi - \pi/2) = 0$ or

$$\phi = \frac{2p + 1}{6}\pi; \quad (25)$$

precisely the same values as for the Parisi equation [16]. For these values of ϕ , the exponential factor in (24) becomes $\cos(3\phi - \pi/2) = \cos(p\pi) = (-1)^n$, giving rise to the left (+1) and right (-1) moving fields respectively. This behaviour is in fact an intrinsic property of the inviscid GOY model, and stem from the quadratic terms and the complex conjugation. This property of selecting specific phases might explain the period-three organisation of the pulses in the forced GOY model as noted by Okkels & Jensen [15].

The simplest case, on which we shall concentrate below, is $p = 1$; a completely imaginary field moving to the right. We thus let $w_n = i\tilde{w}_n$ and dropping the tildes we get the real equation

$$\frac{dw_n}{dt} = -w_{n+1}w_{n+2} + w_{n-1}w_{n-2}. \quad (26)$$

The behaviour of (26) using a cosine-bump as initial condition (19) is shown in Fig. 2. The initial bump splits into a number of pulses with the same shape but different heights. The velocity of each pulse was measured to be $v = 2h$ where h is the height of the pulse. Two pulses can pass through each other after a time delay produced by the collision (Fig. 2, right). These facts seem to indicate that the model (26) is exactly integrable – although, as we shall see later, probably not in terms of analytic functions.

One has to keep in mind that the system is discrete and therefore the shape of a pulse deforms slightly in time. Despite this, one can actually obtain a very precise shape function for the pulse, simply by measuring the field w continuously in time at a given point in the lattice (Fig. 3)

The most characteristic feature of Eq. (22) compared to the original GOY model, is the disappearance of the middle term. It should be noted that other variants of shell models display another limit. An example is the helicity-conserving shell models [19] where in the $r = 1$ limit the right term disappears, while the middle term is preserved. This makes the equation qualitatively different.

4 Pulses in the continuum limit

We shall now show that the continuum limit of (26) is non-trivial and thus that the form of the pulses might be unusual. By expanding w in a Taylor-series and retaining, on the right-hand-side of (26) terms $w^{(p)}w^{(q)}$ with $p + q \leq 3$ we get the continuum limit

$$-w_t = 6ww_x + 6w_xw_{xx} + 3ww_{xxx} \quad (27)$$

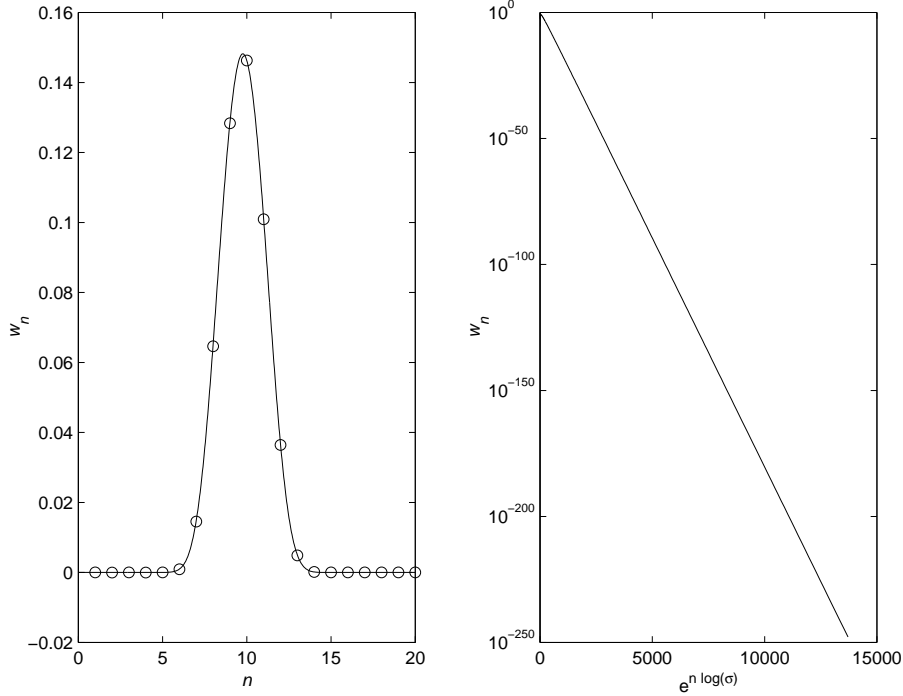


Fig. 3. To the left is shown the shape of the pulse. The circles is the pulse extracted directly (at $t = 210$ in Fig. 2) and the line is the pulse extracted using a time series from one point. On the figure to the right the horizontal axis is $z = \sigma^n$, where $\sigma = 1.618\dots$ is the golden mean. Thus the tail of the pulse fits well to the form $w_n = e^{-az}$.

where again the subscripts denote differentiation.

Using the identity $(w^2)_{xxx} = 6w_x w_{xx} + 2w w_{xxx}$ the continuum model can be written:

$$-w_t = 6w w_x + (w^2)_{xxx} - w w_{xxx} \quad (28)$$

To study the asymptotics, we shall start by omitting the last term. The resulting equation

$$-w_t = 6w w_x + (w^2)_{xxx} \quad (29)$$

strongly resembles the Korteweg de Vries (KdV) equation. We shall refer to it as the Quadratic Korteweg de Vries (QKdV) equation.

4.1 Solitons in the KdV equation

Let us briefly review how the solitons of the KdV equations are found. We look for pulse solutions of the KdV equation

$$w_t = ww_x + w_{xxx} \quad (30)$$

which are only a function of $x \rightarrow x + vt$, so that (30) becomes

$$vw' = ww' + w''' \quad (31)$$

Now we can integrate once to get

$$w'' - vw + \frac{1}{2}w^2 = C_1 \quad (32)$$

Since we are interested in a pulse where the LHS approaches 0 as $x \rightarrow \pm\infty$ we must take $C_1 = 0$. The resulting equation is that of a Newtonian particle moving in time x in the potential

$$V(w) = \int_0^w (-vz + \frac{1}{2}z^2) dz = -\frac{1}{2}vw^2 + \frac{1}{6}w^3 \quad (33)$$

Energy conservation has the form

$$\frac{1}{2}(w')^2 + V(w) = C_2 \quad (34)$$

Again the boundary conditions dictate that $C_2 = 0$ and we can solve (34) as

$$x(w) - x(w_0) = \int_{w_0}^w \frac{dz}{\sqrt{-2V(z)}} \quad (35)$$

This leads to the *sech*² for $w(x)$ but for our purposes the most important point is that the soliton corresponds to the homoclinic orbit starting from the potential hill-top $w = 0$ at $x \rightarrow -\infty$ and returning back at $x \rightarrow -\infty$. The quadratic nature of the hill-top means that the integral for $x(w)$ *diverges* logarithmically for $w \rightarrow 0$ and thus the soliton extends to infinity with an exponential tail in both directions.

4.2 Solitons in the QKdV equation on a vanishing background

We now look for a pulse solutions of (29) and let $x \rightarrow x - vt$, so that (29) becomes

$$vw' = 6ww' + (w^2)''' \quad (36)$$

Again we can integrate once to get

$$(w^2)'' - vw + 3w^2 = C_1 \quad (37)$$

and, if at some (finite or infinite) point the left hand side vanishes, we must take $C_1 = 0$. This means that we are looking for pulses with $w \rightarrow c = 0$. To make a Newtonian problem out of this we now introduce the variable $y = w^2$. Then we get

$$y'' - v\sqrt{y} + 3y = C_1 \quad (38)$$

which is potential motion in the potential

$$V(y) = -\frac{3}{2}by^{3/2} + \frac{3}{2}y^2 \quad (39)$$

where $b = 4v/9$ and the total energy (34) must again be 0. Thus the solution can again be written as (35), but this time the integral converges at $w = 0$ so we can write explicitly for the solution which vanishes at $x = 0$:

$$x(w) = \int_0^y \frac{ds}{\sqrt{-2V(s)}} = \frac{2}{\sqrt{3}} \int_0^w \frac{dz}{\sqrt{bz - z^2}} = \frac{2}{\sqrt{3}} \cos^{-1} \frac{b - 2w}{b} \quad (40)$$

which can be inverted as

$$w = \frac{b}{2} \left(1 - \cos \frac{\sqrt{3}x}{2}\right) = \frac{2v}{9} \left(1 - \cos \frac{\sqrt{3}x}{2}\right) \quad (41)$$

We verify that $w(0) = 0$ but now the solution has support only on the interval $[0, 4\pi]$. Outside of that it is identically zero which means that there is a shock in w_{xx} at those points. The strength of this shock will presumably diminish when higher order approximations to (26) is used. But one can easily see that the term $w w_{xxx}$ which we omitted from (28) will not change this fact (although it will probably alter the simple solution (41)). Closely to the right of $x = 0$, $w(x) \approx \frac{v}{12}x^2$. Thus w_x and $(w^2)_{xxx}$ both go linearly in x (and balance), whereas

$(w^2)_x$ and ww_{xxx} both go like x^3 and do not alter the asymptotics for $x \rightarrow 0^+$. This will be verified explicitly in the next section.

4.3 Higher approximations.

It is possible to take the term ww_{xxx} , which we omitted in (27) explicitly into account [20]. Multiplying (27) with $2w$ on both sides, we can rewrite this as:

$$-(w^2)_t = 4(w^3)_x + 6(w^2w_{xx})_x \quad (42)$$

If we again assume an uniform propagation with constant velocity v , then $w(x, t)$ is only a function of $x - vt$, and the equation above reduces to

$$v(w^2)' = 4(w^3)' + 6(w^2w'')' \quad (43)$$

which can immediately be integrated to yield:

$$w^2(-v + 4w + 6w'') = \text{constant} \quad (44)$$

The non-trivial solution must therefore satisfy

$$6w'' + 4w = v \quad (45)$$

with solution in the form of the “compact” soliton

$$w = \frac{v}{4} \left(1 - \cos \sqrt{\frac{2}{3}}x\right) \quad (46)$$

analogously to (41) but no solutions decaying to 0 at infinity.

This approach is tied to the existence of a conserved energy given by: $E = \int dx w(x, t)^2$, which is conserved only if $2ww_t$ can be written as a total derivative in x :

$$2ww_t = F(w, w_x, \dots)_x \quad (47)$$

But if we furthermore assume a dependence only on $x - vt$, then the above equation reduces to an equation of total derivatives:

$$-v(w^2)' = F(w, w', \dots)' \quad (48)$$

which can be integrated to give:

$$F(w, w', ..) + vw^2 = \text{constant}. \quad (49)$$

To have finite-energy solitons, w must go to zero at infinity. If furthermore $F(w, w', ..)$ goes to zero as w goes to zero, the constant must be zero. We can then divide by w^2 and the equation reduces to

$$\frac{F(w, w', ..)}{w^2} = -v \quad (50)$$

Keeping terms up to 5'th order in the derivatives in equation (26) in the continuum limit, we get:

$$-w_t = 6ww_x + 3ww_{xxx} + 6w_xw_{xx} + \frac{11}{20}ww_{xxxx} + \frac{3}{2}w_xw_{xxx} + 2w_{xx}w_{xxx}. \quad (51)$$

Miraculously, this can be rewritten as

$$-(w^2)_t = \left(4(w^3) + 6(w^2w_{xx}) + \frac{11}{20}w^2w_{xxx} + \frac{2}{5}ww_xw_{xxx} - \frac{2}{5}w_x^2w_{xx} + \frac{4}{5}ww_{xx}^2 \right)_x \quad (52)$$

so that

$$F(w, w', ..) = -4w^3 - 6w^2w_{xx} - \frac{11}{20}w^2w_{xxx} - \frac{2}{5}ww_xw_{xxx} + \frac{2}{5}w_x^2w_{xx} - \frac{4}{5}ww_{xx}^2 \quad (53)$$

Equation (50) is then:

$$\begin{aligned} v &= 4w + 6w'' + \frac{11}{20}w'''' + \frac{2}{5} \frac{w'w'''}{w} + \frac{2w''^2}{5} - \frac{2}{5} \frac{w'^2w''}{w^2} \\ &= 4w + 6w'' + \frac{11}{20}w'''' + \frac{2}{5} \left(\frac{w'^2w''}{w} \right)' \frac{1}{w'} \end{aligned} \quad (54)$$

which might have non-trivial soliton-solutions as long as the last term equals v at large $x - vt$. So for large $x - vt$, we must have:

$$\frac{5}{2}vw' = \left(\frac{w'^2w''}{w} \right)' \quad (55)$$

or, by integration:

$$\frac{5}{2}vw = \frac{w'^2w''}{w} - C \quad (56)$$

where C is some integration-constant. Now multiply this with $w w'$:

$$\frac{10}{3}v(w^3)' + 2C(w^2)' = (w'^4)' \quad (57)$$

and integrate again

$$\frac{10}{3}vw^3 + 2Cw^2 = w'^4 \quad (58)$$

where no extra constant arises, because of the boundary-condition at infinity. Thus

$$w' = \left(\frac{10v}{3}w^3 + 2Cw^2 \right)^{1/4} \quad (59)$$

If $C \neq 0$, the 2nd term dominates asymptotically, and we get $w(x, t) \sim (x-vt)^2$ for large $x - vt$. On the other hand if $C = 0$ then $w(x, t) \sim (x - vt)^4$ for large $x - vt$. In both cases $w(x, t)$ does not decay to zero as $x - vt$ goes to infinity. So again there are no soliton-solutions, that decay to zero at infinity.

4.4 Solitons in the QKdV with $c > 0$.

The strange appearance of the solitons is closely linked to the fact that w decays to zero asymptotically. If $w \rightarrow c > 0$ for $x \rightarrow \pm\infty$, the pulse will decay exponentially to this value far away just as in the KdV case. The difference is that the constant C_1 now no longer vanishes. Instead $C_1 = -vc + c^2$ and the potential acquires the form

$$V(y) = -\frac{1}{2}by^{3/2} + \frac{1}{2}y^2 - C_1y \quad (60)$$

Now, for $v > 0$ and small $c > 0$, $C_1 \approx -vc < 0$ so the potential acquires a small hill top at $w = c$. This hill top is non singular (albeit in a very small region) and we get back to the usual situation (like KdV) where the soliton spreads over the entire region with an exponential tail. Near $w = c$ we get from (35)

$$x(y) - x(y_0) = \int_{y_0}^y \frac{ds}{\sqrt{-(s-c)^2 V''(c)}} = \frac{1}{\sqrt{-V''(c)}} \log \frac{y-c}{y_0-c} \quad (61)$$

where $V''(c) = -\frac{v}{2c}$. Thus the solution decays as

$$y(x) = w^2(x) = c + (y_0 - c)e^{\alpha x} \quad (62)$$

where $\alpha = \sqrt{-V''(c)} \sim (\sqrt{c})^{-1}$. Thus the decay length $\xi \sim \sqrt{c}$.

5 Asymptotics of solitons in the discrete model

The results obtained in the continuum limit in the previous section are not born out by simulations. The pulses do not seem to have compact support, but decay far away. The decay is not exponential, but seems to be more rapid. We shall now give an estimate of this decay and subsequently try to refine it.

Let us approximate the derivative in (26) as $w'(x) \approx w(x+1) - w(x)$. Further, expecting a rapid decay, we shall neglect $w(x+1)$ and $w(x+2)$ compared to $w(x)$, $w(x-1)$ and $w(x-2)$. Thus we simplify (26) to

$$w(x) = w(x-1)w(x-2) \quad (63)$$

Now let $\zeta(x) = \log(w(x))$ whereby we find

$$\zeta(x) = \zeta(x-1) + \zeta(x-2) \quad (64)$$

This recursion relation is identical to the one for the Fibonacci numbers, and in general $\zeta(x)$ will grow like σ^x . To determine σ , assume that

$$\zeta(x) = a\sigma^x \quad (65)$$

which should be valid at large x . Inserting into (64) gives us

$$\sigma^2 - \sigma - 1 = 0 \quad (66)$$

with the (positive) solution

$$\sigma = \frac{1}{2}(1 + \sqrt{5}) \quad (67)$$

the so-called *golden mean*. This gives the extremely rapid decay

$$w(x) \approx e^{-a\sigma^x} \quad (68)$$

with some positive constant a . This rather unusual behaviour is extremely well represented by the numerical solution (Fig. 3).

To refine this, assume that

$$w(x) = f(x)e^{a\sigma^x} \quad (69)$$

Inserting this into (26) and cancelling a factor of $e^{a\sigma^x}$ (using (67)) we get

$$af(x)\sigma^x \log \sigma - f'(x) = f(x-1)f(x-2) - f(x+1)f(x+2)e^{-da\sigma^x} \quad (70)$$

where $d = \sigma + \sigma^2 - \sigma^{-1} - \sigma^x - 2 \approx 3.2 > 0$. If the function $f(x)$ is “reasonable” the last term can be dropped and we get

$$af(x)\sigma^x \log \sigma - f'(x) = f(x-1)f(x-2) \quad (71)$$

and we can get the asymptotic behaviour $f \sim \sigma^x$ by matching the first term on the left hand side to the right hand side. Thus $f(x) \approx c\sigma^x$ with $c = a\sigma^3 \log \sigma$ and the solution takes the form

$$w(x) = a\sigma^{(x+3)} \log \sigma e^{a\sigma^x} = a \log \sigma e^{(x+3) \log \sigma + a\sigma^x} \quad (72)$$

Note that a is still not determined and we presumably need to solve for the whole soliton structure to get this constant.

6 Expansion for non-zero background

As seen in section 5 pulses converging to $c_0 > 0$ decay exponentially. This is born out by our numerics and we now give a method to obtain the asymptotic behaviour of a pulse solution.

We consider

$$\dot{w}_n = w_{n+1}w_{n+2} - w_{n-1}w_{n-2}. \quad (73)$$

For the field $w_n(t)$ we make the expansion

$$w_n(t) = \sum_{s=0}^{s=\infty} c_s \exp(-s(kn - vt)). \quad (74)$$

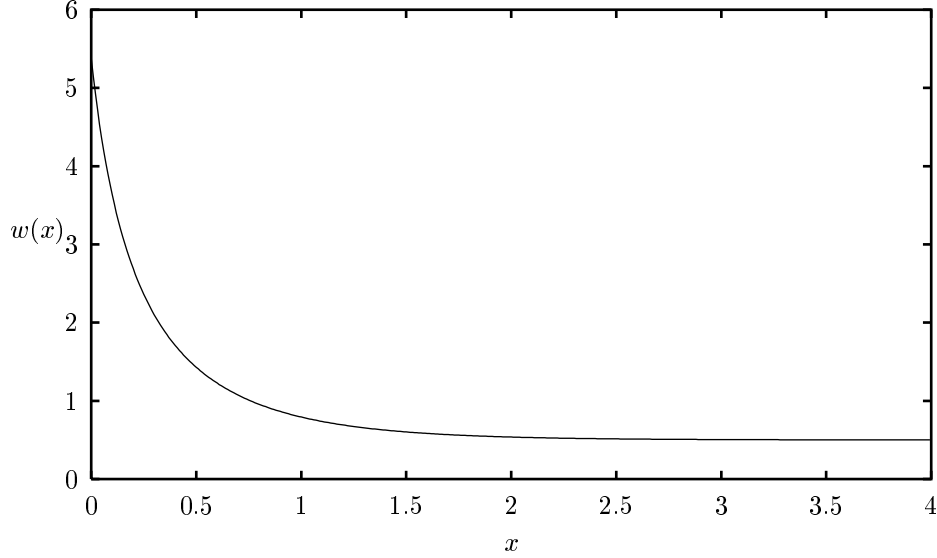


Fig. 4. An example of an “exact” solution of a pulse using the expansion Eq. (74) with the coefficients obtained by the recursion relation Eq. (76) with $k = 2$, $c_0 = 0.5$ and $c_1 = 2$. Note that w_n asymptotically approaches c_0 .

Hence we have

$$v \sum_{l=1}^{\infty} l c_l \exp(-l(kn - vt)) = -2 \sum_{l=1}^{\infty} \exp(-l(kn - vt)) \sum_{s=0}^l c_s c_{l-s} \sinh(2lk - sk). \quad (75)$$

Thus we have the recursion relation

$$c_l(vl - 2c_0 \sinh(2lk) - 2c_0 \sinh(lk)) = -2 \sum_{s=1}^{l-1} c_s c_{l-s} \sinh(2lk - sk). \quad (76)$$

Although the recursion relation is non-linear, it turns out that it can be solved successively in terms of the two constants c_0 and c_1 . For $l = 1$ we get

$$v = 2c_0(\sinh k + \sinh 2k), \quad (77)$$

giving a relation between the constant background c_0 , the width k , and the velocity v . For $l = 2$ we obtain

$$c_2 = c_1^2 \frac{2 \sinh 3k}{2v - 2c_0 \sinh 2k - 2c_0 \sinh 4k}. \quad (78)$$

Similarly, for $l = 3$ we get

$$c_3 = 4c_1^3 \frac{(\sinh 5k + \sinh 4k) \sinh 3k}{(3v - 2c_0 \sinh 6k - 2c_0 \sinh 3k)(2v - 2c_0 \sinh 4k - 2c_0 \sinh 2k)}. \quad (79)$$

It is straightforward, but tedious, to continue this calculation (we have computed c_4 and c_5).

To show that (74) is a solution, we need to show that the coefficients c_l obtained from the recursion relation (76) are such that the sum in (74) is either convergent or Borel summable. We have not succeeded in this in general. However, it is possible to show convergence when the width k is large, and also presumably when k is small. Let us consider k to be large. The velocity then becomes

$$v \approx c_0 e^{2k} + O(e^k). \quad (80)$$

From the recursion relation (76) we get a solution of the form

$$c_l \approx c_1^l e^{-k(l-1)} / c_0^{l-1} (1 + O(e^{-k})). \quad (81)$$

The corresponding asymptotic solution can be found by performing the sum in (74),

$$w_n(t) \approx \frac{c_0 + c_1 e^{-kn + c_0 t \exp 2k}}{1 - (c_1/c_0) e^{-k(n+1) + c_0 t \exp 2k}}. \quad (82)$$

Numerically, one can easily generate an “exact” solution by Eq. (74) using the recursion relation Eq. (76). Of course the solution exists only if the coefficients c_s converge. We have observed that the radius of convergence in parameter space has a “hole” around the point $c_0 = 0, c_1 = 0$. This is not surprising because this expansion is only valid on non-zero background and from the structure of the recursion relations it is clear that $c_0 = c_1 = 0$ leads to a trivial case where $c_s = 0$ for all s . Away, from the open set around $c_0 = c_1 = 0$ we find a very fast convergence of the series. An example of the obtained solution is shown in figure 4.

Note that formally we can apply this expansion also to the case treated in section 6, where $w \rightarrow 0$ for $r \rightarrow \infty$: At first sight this seems to require $c_0 = 0$, which doesn’t work. However one has to keep in mind that the results of the previous section shows that in this case k must be negative, indeed $k = -\log \sigma$ and this means that we have an expansion in terms of *growing* exponentials. The background value c is therefore not given simply by c_0 in this limit, but all higher terms will contribute to it.

7 Acceleration of solitons for $r > 1$

When r is slightly above unity, the main difference between our zero-spacing model and the real GOY model seems to be the acceleration of the bursts seen e.g. in Fig. 1. Letting $r = 1 + \epsilon$ in (21) and retaining helicity conservation ($\delta = 1 - 1/r \approx \epsilon$) we see that our inviscid model (22), in lowest order of ϵ , becomes

$$\frac{dw_n^*}{dt} = -i(w_{n+1}w_{n+2} - w_{n-1}w_{n-2} - 4\epsilon w_n^2) \quad (83)$$

For purely imaginary w this is

$$\frac{dw_n}{dt} = -w_{n+1}w_{n+2} + w_{n-1}w_{n-2} + 4\epsilon w_n^2 \quad (84)$$

In the continuum limit, neglecting all higher order derivatives we get

$$\frac{\partial w}{\partial t} = -6ww_x + 4\epsilon w^2 \quad (85)$$

from which we clearly see the acceleration caused by the last term. Note that this equation preserves energy conservation in the form $E = \int u^2 dx = \text{const}$, but now we have to remember the transformation leading to (21), i.e. $u = wk$, where $k = k_0(1 + \epsilon)^n \approx k_0 e^{\epsilon x}$. Thus (85) can be written

$$\frac{\partial}{\partial t}(w^2 e^{-2\epsilon x}) = -\frac{\partial}{\partial x}(4w^3 e^{-2\epsilon x}) \quad (86)$$

which shows that the appropriate shock-condition is

$$V = \frac{[4w^3 e^{-2\epsilon x}]}{[w^2 e^{-2\epsilon x}]} \quad (87)$$

where V is the velocity of the shock and $[f(x)]$ denotes the discontinuity of the quantity x across the shock. Since w vanishes on one side of the shock we get

$$V = 4w \quad (88)$$

The characteristic equations for (85) are

$$\frac{dx}{dt} = 6w \quad (89)$$

and

$$\frac{dw}{dt} = 4\epsilon w^2 \quad (90)$$

The latter can be integrated as

$$w = \frac{w_0}{1 - 4\epsilon w_0 t} \quad (91)$$

where w_0 is the initial field taken as a function of the initial coordinate x_0 . The second characteristic equation can now be integrated as

$$x = x_0 - \frac{3}{2\epsilon} \log(1 - 4\epsilon w_0 t) \quad (92)$$

Thus each characteristic ends in a singularity at time $t = 1/4\epsilon w_0(x_0)$. Never the less it is perhaps not obvious that the shocks also have to end in a singularity at a finite time. To investigate this, we must investigate the shock condition together with the solutions (91) and (92). The shock velocity is $V = dx_e/dt$, where x_e is the edge of the shock. The natural variable is however x_0 and we thus express the shock-condition as

$$4w = V = \frac{dx}{dt} = \frac{\partial x}{\partial x_0} \frac{dx_0}{dt} + \frac{\partial x}{\partial t} \quad (93)$$

On performing the differentiations of (92) with x_0 and t and inserting the solution (91) for w we get

$$\left[1 + \left(6\frac{\partial w}{\partial x_0} - 4\epsilon w_0\right)t\right] \frac{dx_0}{dt} = -2w_0 \quad (94)$$

To make further progress we must know the form of w_0 . In our simulations of bursts, we took distributions like (41), which are strictly zero outside the interval $[x_1, x_2]$ and approach the ends of the interval with zero slope. Thus, close to x_1 (which must dominate at large times) the form will be

$$w_0 \approx a(x_0 - x_1)^2 \quad (95)$$

With this assumption (94) becomes:

$$(1 + 4ay(3 - \epsilon y)t) \frac{dy}{dt} = -2ay^2 \quad (96)$$

where $y = x_0 - x_1$. When $t \rightarrow \infty$ and $y \rightarrow 0$ the parenthesis on the left hand side must be dominated either by the term proportional to t or by the constant. If we assume that $4ay(3 - \epsilon y)t \rightarrow 0$ we get the simple equation

$$\frac{dy}{dt} = -2ay^2 \quad (97)$$

with the solution

$$y = (c + 2at)^{-1} \quad (98)$$

where $c = 1/y_0$. With this solution, however, $4ay(3 - \epsilon y)t \rightarrow 6$ in contradiction to the assumption. Therefore we must assume that yt does not decay to zero and the dominant terms are now

$$3t \frac{dy}{dt} = -y \quad (99)$$

which gives the decay $y \sim t^{-1/3}$. This solution doesn't work either, since the solution (91) only makes sense asymptotically if $ty^2 \rightarrow 0$ as $t \rightarrow \infty$. We therefore conclude that, within the approximation leading to the continuum limit (85), the position of the shock will diverge to infinity at a finite time. It is not clear whether this behaviour is seen in the discrete equation as well(84).

It is then clear that a pulse reach the dissipative range in finite time. This behaviour is qualitative the same as was found for the Parisi equation.

8 Lyapunov exponents

In this section we study the Lyapunov exponents of the GOY model in the limit of $r \rightarrow 1$. Since we aim at keeping the size of the inertial range fixed, the number of shells must also be varied as a function of r , if the ‘‘external’’ parameters, i.e., viscosity and forcing are kept fixed at $\nu = 10^{-6}$, $k_0 = 2^{-4}$, $f = (1+i)0.005$. For $r = 2$ these parameters correspond to $N = 19$ shells; therefore we use a dependence between N and r as:

$$N = 8 + \left[11 \frac{\log(2)}{\log(r)} \right] \quad (100)$$

where the brackets stand for integer value. We wish to quantify the ‘‘strength’’ of the intermittency as a function of the effective shell spacing r . One way to do this is by means of the maximal Lyapunov exponent [21]. To compute the

maximal Lyapunov exponent in the GOY model, we introduce the notation $\mathbf{U} \equiv (Re(u_1), Im(u_1), \dots, Re(u_N), Im(u_N))$ and $F_i = dU_i/dt$ and consider the linear variational equations

$$\frac{dz_i}{dt} = \sum_{j=1}^{2N} A_{ij} \cdot z_j \quad i = 1, \dots, 2N \quad (101)$$

for the time evolution of an infinitesimal increment $\mathbf{z} = \delta\mathbf{U}$, where

$$A_{nj} \equiv \partial F_n / \partial U_j \quad (102)$$

is the Jacobian matrix of Eqs. (1). The solution for the tangent vector \mathbf{z} can thus be formally written as $\mathbf{z}(t_2) = \mathbf{M}(t_1, t_2) \cdot \mathbf{z}(t_1)$, with $\mathbf{M} = \exp \int_{t_1}^{t_2} \mathbf{A}(\tau) d\tau$. A generic tangent vector $\mathbf{z}(t)$ is projected by the evolution along the eigenvector $\mathbf{e}^{(1)}$, belonging to the maximum Lyapunov exponent, i.e. $\mathbf{z}(t) = |\mathbf{z}(0)| \mathbf{e}^{(1)} \exp(\lambda_1 t)$ leading to

$$\lambda_1 = \lim_{t \rightarrow \infty} \frac{1}{t} \ln \frac{|\mathbf{z}(t)|}{|\mathbf{z}(0)|} \quad (103)$$

where $\mathbf{z}(0)$ is the initial tangent vector.

Practically, Eqs. (1, 101) are integrated simultaneously over a certain time δt , starting with a normalised tangent vector in a random direction, $\hat{\mathbf{z}}(0)$. The increment over time δt in the length of the tangent vector is then $\delta z_1 = |\mathbf{z}(\delta t)| / |\hat{\mathbf{z}}(0)|$. Next, the tangent vector is normalised $\hat{\mathbf{z}}(\delta t) = \mathbf{z}(\delta t) / |\mathbf{z}(\delta t)|$ and this vector is used as a seed for a new integration over the time δt i.e. propagated forward to $t = 2\delta t$. Generalising this argument we obtain the i 'th increment $\delta z_i = |\mathbf{z}(i\delta t)| / |\hat{\mathbf{z}}((i-1)\delta t)|$ and the maximal Lyapunov exponent is given by (where we now set $\lambda = \lambda_1$):

$$\lambda = \lim_{M \rightarrow \infty} \frac{1}{M} \sum_{i=1}^M \frac{\ln(\delta z_i)}{\delta t} \quad (104)$$

We have followed two paths for the values of the parameters a_n, b_n, c_n . In the first, the constraint Eq. (5) is applied, and in the other we keep the parameters fixed at the canonical values $a_n = 1, b_n = c_n = -\frac{1}{2}$. The results of the numerical simulations are shown in Fig. 5. In both cases we observe that the maximal Lyapunov exponent appears to vanish in the limit $r \rightarrow 1$ (the minimal value of r in the plot is 1.004, corresponding to ~ 1000 shells). The lower curve is the one related to the conservation of both energy and helicity. The maximal Lyapunov exponent remains in this case nearly constant in a large interval of r -values and then finally drops to zero. In the case where only

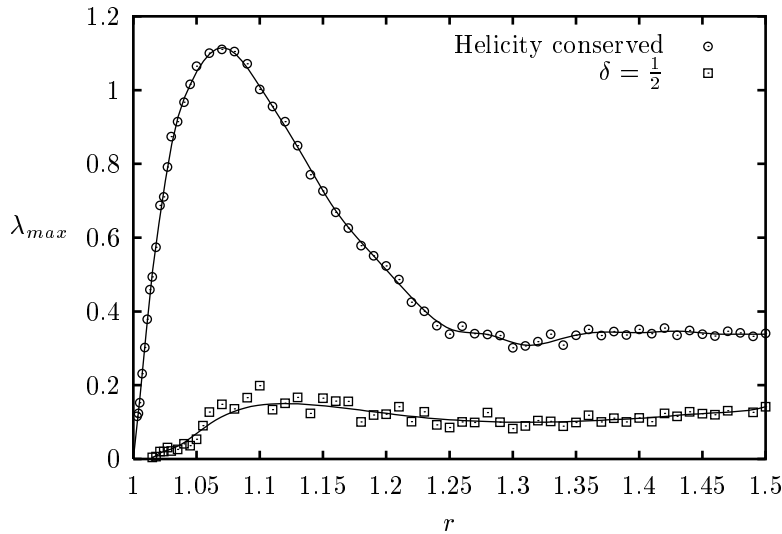


Fig. 5. The maximum Lyapunov exponent λ_{max} for a case with conservation of helicity (i.e. $\delta = 1 - 1/r$) and where δ is fixed at $1/2$. The solid line is an interpolation to guide the eye.

energy is conserved (the upper curves) there is a maximum around $r = 1.1$ after which also this decreases towards zero. Based on these numerical results we conclude that the GOY model does not exhibit chaotic dynamics in the zero-spacing limit. Similar behavior has been observed recently in a shell model containing two fields [22]. Here it has been observed [23] that the intermittency corrections disappear in the limit $r \rightarrow 1$.

9 Conclusions

The main objective of this paper is to study the dynamical behavior of single burst motion on a vanishing background in various shell models. The motion of single bursts is important for the understanding of intermittent behavior in turbulence. Indeed it is believed that the presence of intermittency causes the corrections to the classical Kolmogorov theory which manifest itself as multiscaling of higher order structure functions. In the present paper we have studied the motion of a single burst in three different versions of shell models:

- (1) The standard GOY model when the shell spacing approaches, but is different, from zero;
- (2) The Parisi continuum limit of the GOY model;
- (3) The zero-spacing of the GOY model where helicity conservation is kept.

In all cases we observe that an initial disturbance splits up in a left- and a right-moving part. In case 1) the pulse retains its shape and whereas the right moving part accelerates, the left-moving part decelerates. In case 2) an initial disturbance splits into left- and right-moving shocks. The right-moving shock accelerates and its position diverges to infinity in a finite time. Finally, in case 3) the shape retains its “solitary” form and does not turn into a shock. Here the velocity also remains constant and the solitons pass through each other with a slight phase shift but without changing their shapes, completely as found in integrable field theories.

We have analytically calculated the motion of the shocks in case 2) by means of characteristics. In case 3) we have analytically estimated the asymptotic shape of the solitary wave and find that it decreases super exponentially with a decay constant given by the golden mean. On a non-vanishing background we have on the other hand found that the decay of the soliton is a standard exponential. From numerical simulations in case 1), we have estimated the maximal Lyapunov exponent and found that it vanishes in the limit of zero-spacing, although the the motion remains chaotic for finite spacing. This results is expected since, as we have shown earlier, the continuum Parisi limit resembles the Burgers equation and gas theory and is in fact exactly soluble by the method of characteristics.

We hope that our findings could be a starting point for a more detailed understanding of structure of intermittency, in particular of how the presence of isolated bursts give rise to corrections to classical scaling.

References

- [1] E. B. Gledzer, *Sov. Phys. Dokl.* **18**, 216 (1973).
- [2] M. Yamada and K. Ohkitani, *J. Phys. Soc. Japan* **56**, 4210(1987); *Prog. Theor. Phys.* **79**,1265(1988).
- [3] M. H. Jensen, G. Paladin, and A. Vulpiani, *Phys. Rev. A* **43**, 798 (1991).
- [4] R. Benzi, L. Biferale, and G. Parisi, *Physica D* **65**, 163 (1993).
- [5] D. Pisarenko, L. Biferale, D. Courvasier, U. Frisch, and M. Vergassola, *Phys. Fluids A* **65**, 2533 (1993).
- [6] L. Kadanoff, D. Lohse, J. Wang, and R. Benzi, *Phys. Fluids* **7**, 617 (1995).
- [7] L. Kadanoff, D. Lohse, and N. Schörghofer, *Physica D* **100**, 165 (1997).
- [8] N. Schörghofer, L. Kadanoff, and D. Lohse, *Physica D* **88**, 40 (1995).
- [9] L. Biferale, A. Lambert, R. Lima, and G. Paladin. *Physica D* **80**, 105 (1995).

- [10] T. Bohr, M. H. Jensen, G. Paladin, and A. Vulpiani, *Dynamical systems approach to turbulence* (Cambridge University Press, Cambridge), 1998.
- [11] E. Siggia, *Phys. Rev. A* **17**, 1166 (1978).
- [12] G. Parisi. A mechanism for intermittency in a cascade model for turbulence. Preprint of the University of Rome II. Unpublished, 1990.
- [13] P. Ditlevsen. Temporal intermittency and cascades in shell models of turbulence. *Phys. Rev. E*, 54:985–988, 1996.
- [14] T. Dombre and J.-L. Gilson, *Physica D* **111**, 265 (1998); J.-L. Gilson and T. Dombre, *Phys. Rev. Lett.* **79**, 5002 (1997); I. Daumont, J.-L. Gilson and T. Dombre, *chao-dyn/9905017* (1999).
- [15] F. Okkels and M.H. Jensen, *Phys. Rev. E* **57**, 6634 (1998).
- [16] K. H. Andersen, T. Bohr, M. H. Jensen, and P. Olesen. Proceeding of international conference on disorder and chaos in honour of Giovanni Paladin. *J. Phys. IV France*, 8:121–130, 1998.
- [17] F. Anselmet, Y. Gagne, E.J. Hopfinger and R.A. Antonia, *J. Fluid Mech.* **140**, 63 (1984).
- [18] J. Herweijer and W. van de Water, *Phys. Rev. Lett.* **74**, 4653 (1995).
- [19] R. Benzi, L. Biferale, R.M. Kerr and E. Trovatore, *Phys. Rev. E* **53**. 3541 (1996).
- [20] We would like to thank Ola Tornkvist and Conor Houghton for pointing this out to us.
- [21] J. Kockelkoren, F. Okkels, and M.H. Jensen. *J. Stat. Phys.*, 93:833–842, 1998.
- [22] L. Biferale and R. Kerr, *Phys. Rev. E* **52**, 6113 (1995).
- [23] R. Benzi, L. Biferale and E. Trovatore, *Phys. Rev. Lett.* **77**, 3114 (1996).